Cellular and Molecular Life Sciences (2022) 79:564
https://doi.org/10.1007/s00018-022-04600-y

ORIGINAL ARTICLE

Cannabidiol as a modulator of α7 nicotinic receptors

Juan Facundo Chrestia[1] · María del Carmen Esandi[1] · Cecilia Bouzat[1]

Received: 2 July 2022 / Revised: 29 September 2022 / Accepted: 14 October 2022

Abstract

Cannabidiol (CBD), an important terpenoid compound from marijuana with no psychoactive effects, has become of great pharmaceutical interest for several health conditions. As CBD is a multitarget drug, there is a need to establish the molecular mechanisms by which CBD may exert therapeutic as well as adverse effects. The α7 nicotinic acetylcholine receptor (α7 nAChR) is a cation-permeable ACh-gated channel present in the nervous system and in non-neuronal cells. It is involved in different pathological conditions, including neurological and neurodegenerative disorders, inflammation, and cancer. By high-resolution single-channel recordings and confocal microscopy, we here reveal how CBD modulates α7 nAChR ionotropic and metabotropic functions. CBD leads to a profound concentration-dependent decrease of α7 nAChR single-channel activity with an IC_{50} in the sub-micromolar range. The inhibition of α7 nAChR activity, which takes place through a membrane pathway, is neither mediated by receptor phosphorylation nor overcome by positive allosteric modulators and is compatible with CBD stabilization of resting or desensitized α7 nAChR conformational states. CBD modulation is complex as it also leads to the later appearance of atypical, low-frequency α7 nAChR channel openings. At the cellular level, CBD inhibits the increase in intracellular calcium triggered by α7 nAChR activation, thus decreasing cell calcium responses. The modulation of α7 nAChR is of pharmacological relevance and should be considered in the evaluation of CBD potential therapeutic uses. Thus, our study provides novel molecular information of CBD multiple actions and targets, which is required to set the basis for prospective applications in human health.

Keywords Nicotinic receptor · Patch-clamp · Single-channel recordings · Cannabinoids · Cys-loop receptors

Abbreviations

nAChR	Nicotinic acetylcholine receptor
ACh	Acetylcholine
ICD	Intracellular domain
5-HI	5-Hydroxyindole
PNU-120596	N-(5-Chloro-2,4-dimethoxyphenyl)-N′-(5-methyl-3-isoxazolyl)-urea
CBD	Cannabidiol
THC	Trans-Δ^9-tetrahydrocannabinol
α-BTX	α-Bungarotoxin
ECS	Extracellular solution
nP_o	Fraction of time in the open state

Introduction

Cannabis sativa plant extracts contain a large number of structurally related, highly lipophilic terpenoid derivatives known as phytocannabinoids [1]. The plant, known commonly as marijuana, is widely popular as a recreative drug due to its ability to induce psychological and euphoric states in individuals, an effect mainly due to the presence of the cannabinoid compound trans-Δ^9-tetrahydrocannabinol (THC). However, *Cannabis sativa* has long history as a medicinal plant. Recently, there has been considerable interest in its therapeutic potential for patients with a variety of medical conditions, including pain, cancer, neurological and neurodegenerative disorders [2–4]. Cannabidiol (CBD), which is the second most abundant cannabinoid compound, has become of great pharmaceutical interest. In contrast to THC, CBD does not produce psychoactive effects [3].

In vitro and in vivo studies have indicated that CBD can be used in the treatment of various neurological conditions, such as neuropathic pain, epilepsy, and brain damage from stroke [5–7]. CBD-based therapies have been recently

✉ Cecilia Bouzat
inbouzat@criba.edu.ar

[1] Departamento de Biología, Bioquímica y Farmacia, Instituto de Investigaciones Bioquímicas de Bahía Blanca, Universidad Nacional del Sur-Consejo Nacional de Investigaciones Científicas y Técnicas (CONICET), Camino La Carrindanga Km 7, 8000 Bahía Blanca, Argentina

legalized for the treatment of epilepsy (and other medical conditions) in children and adults in several countries [1, 3, 8, 9]. CBD has very low affinity for endogenous cannabinoid receptors, and the current evidence suggests that it does not directly interact with the endocannabinoid system except at supraphysiological concentrations [10, 11]. Therefore, its beneficial effects appear to be mediated by other receptor targets.

Thus, as further evidence for CBD's potential beneficial effects for diverse pathological situations emerges, there is an urgent need to establish the molecular targets by which CBD exerts its therapeutic or adverse effects. In this regard, several targets, including ion channels, G-protein coupled receptors, and Cys-loop receptors, have been proposed [12, 13].

Cys-loop receptors are pentameric ligand-gated ion channels involved in chemical synapses throughout the peripheric and central nervous systems and are also present in non-neuronal cells. In vertebrates, they are anionic channels activated by GABA or glycine, and cationic channels activated by ACh (nicotinic receptors, nAChRs) or serotonin (5-HT_3 receptors) [14].

Several reports have shown modulation of Cys-loop receptors by phytocannabinoids and endocannabinoids independent of cannabinoid receptors with potential physiological or therapeutic consequences. It has been reported that exogenous and endogenous cannabinoids potentiate glycine receptors in a subunit-specific manner [15–18]; CBD and THC allosterically inhibit 5-HT_3A macroscopic responses [19, 20]; the endocannabinoid 2-arachidonoyl glycerol (2-AG), THC and CBD potentiate $GABA_A$ receptors [21, 22]. With respect to α7 nAChR, it has been reported that anandamide, 2-AG, R-methanandamide, and CBD allosterically decrease macroscopic responses in oocytes and that CBD decreases choline-evoked currents in rat hippocampal slices [23–25].

α7 nAChR shows high calcium permeability and the fastest desensitization among nAChRs [14]. In addition to its ionotropic actions, α7 nAChR induces the release of calcium from intracellular stores and triggers signaling pathways [26, 27]. α7 nAChR is one of the most abundant nAChRs in the nervous system. It is highly expressed in cortex, hippocampus, and subcortical limbic regions and contributes to cognition, attention, and memory. It regulates the release of neurotransmitters, mediates fast synaptic transmission, and modulates neuronal excitability [28–30]. Its dysfunction has been associated with several neurological and neurodegenerative disorders, such as schizophrenia, autism, and Alzheimer's disease [31, 32]. α7 nAChR is also expressed in non-neuronal cells, including astrocytes, microglia, and immune cells, where it contributes to anti-inflammatory and neuroprotective effects. Therefore, α7 nAChR potentiation has emerged as a therapeutic strategy for neurological, neurodegenerative and inflammatory disorders [14, 33, 34]. On the other hand, increased α7 nAChR activity in certain cells may contribute to cancer progression via promotion of cell proliferation, apoptosis inhibition and tumor angiogenesis stimulation [35, 36].

Given the relevant functions of α7 nAChR in physiological and pathological situations, deciphering the molecular basis of the effects of phytocannabinoids on this receptor is of importance due to the progressive interest in their establishment as therapeutic drugs. Here, we revealed from a molecular perspective how CBD modulates integrated cell responses mediated by α7 nAChR activation, including single channel currents and intracellular calcium signaling.

Materials and methods

Chemicals

Compounds purchased from commercial sources were as follows: probenecid from Santa Cruz Biotechnology (USA), PNU-120596 from Tocris Bioscience (UK), α-bungarotoxin from Invitrogen (USA), 5-hydroxyindol, acetylcholine and atropine from Merck (USA); Fluo-3AM (Molecular Probes, USA). The stock CBD solution (in ethanol) was kindly provided by Drs. Fernando J. Sepulveda and Gonzalo Yevenes (Universidad de Concepción, Chile). CBD (99.56 wt%) was identified as the only phytocannabinoid present in the sample by convergence chromatography compared to reference standards (ProVerde Laboratories, USA). Delta-9-tetrahydrocannabinol (THC) was kindly provided by Dr. Susana Pasquaré (Instituto de Investigaciones Bioquímicas de Bahía Blanca, CONICET) and corresponded to the standard THC (Cerilliant Corporation).

Cell culture

BOSC-23 cells derived from HEK-293 cells (kindly provided by Dr. Sine, Mayo Clinic, USA) were cultured with Dulbecco's Modified Eagle's Medium (DMEM) culture medium (GIBCO, USA) supplemented with 100 µg/mL streptomycin–100 IU/mL penicillin (Invitrogen, USA), 10% fetal bovine serum (Internegocios, Argentina).

Receptor expression and mutations

Human α7 nAChR cDNA subunit was subcloned into the pRBG4 expression vector [37]. Mutant α7 nAChRs were: α7-Y386F/Y442F, which is a double mutant receptor lacking tyrosine residues in the intracellular domain (ICD) [38]; α7-TSLMF, which carries five mutations in different transmembrane domains (S223T and A226S in M1, M254L in M2, and I281M and V288F in M3) and is insensitive

to PNU-120596 and other PAMs [39–41]; α7-S365A and α7-T331A, which carry mutations of serine or threonine to alanine residues located in the ICD. The mutations were carried out using the Quick-Change kit (Stratagene, USA) and were confirmed by sequencing (Macrogen Inc., South Korea).

BOSC-23 cells were transfected by the calcium phosphate procedure with wild type or mutant α7 subunit cDNAs together with the α7 nAChR chaperone cDNAs, Ric-3 and NACHO, using a cDNA ratio α7:Ric-3:NACHO 1:2:1 and total amount of cDNA of 5 μg/35 mm dish; green fluorescence protein (GFP) cDNA plasmid was used to allow identification of transfected cells [38, 42]. All transfections were carried out for about 8–12 h in DMEM with 10% fetal bovine serum. Cells were used for experiments two to three days after transfection [37, 42].

Single-channel recordings

Single channels were recorded in the cell-attached or inside-out patch configurations as described before [37, 41–43]. The extracellular solution (ECS) and pipette solutions contained 142 mM KCl, 5.4 mM NaCl, 1.8 mM $CaCl_2$, 1.7 mM $MgCl_2$ and 10 mM HEPES (pH 7.4). Single-channel currents were digitized at 5–10 μs intervals and low-pass filtered at a cut-off frequency of 10 kHz using an Axopatch 200B patch-clamp amplifier (Molecular Devices, USA). Analysis was performed with the program TAC (Bruxton Corporation, Seattle, USA) with the Gaussian digital filter at 9 kHz (Final cut-off frequency 6.7 kHz). For recordings with ACh and PNU-120596, the filter was set at 3 kHz to facilitate the analysis. TAC detects events by searching the data to find a threshold crossing. An estimate of the channel amplitude is used to set the threshold level. Every crossing of the threshold is interpreted as the opening or closing of the channel. We used the half-amplitude threshold criterion; thus, if the amplitude value crosses the 50% value of the estimated amplitude, the event starts, and when the data value crosses threshold in the opposite direction, the event ends [44]. To determine channel amplitude, events were tracked regardless of current amplitude and amplitude histograms for events longer than 0.3 ms were constructed and fitted by a Gaussian function [43]. Open-time histograms were fitted by the sum of exponential functions by maximum likelihood using the program TACFit (Bruxton Corporation, USA). Bursts of channel openings were identified as a series of closely separated openings preceded, followed by closings longer than a critical duration, which was taken as the point of intersection between closed components as previously described [37, 41, 45]. Critical durations were defined by the intersection between the first and second briefest components in the closed-time histogram for bursts of α7 activated by ACh (~ 200–500 μs). For defining bursts in the presence of 5-HI, critical times were selected between the second and third closed components (~ 1–3 ms) [37, 43, 45]. In the presence of PNU-120596 and ACh, the critical time for defining clusters was determined by the point of intersection between the third and fourth closed components which allows a clear separation of clusters (~ 30–60 ms) [45]. The mean open duration (τ_{open}) and the mean burst duration (τ_{burst}) were taken from the slowest components of the corresponding histograms. The fraction of time that the channel is in the open state (nPo) was determined only for experiments in which the drug was added during the recording to discard variations in receptor expression level among different patches. It corresponded to the total time that the channel is open/total time of the recording analyzed and was determined in the same recording for the same period of time before and after addition of the drug.

For measuring the effects of CBD on α7 nAChR from cell-attached patches, two different strategies were followed. In one strategy, CBD (at the desired final concentration) was added to the pipette solution together with ACh. In the other strategy, single-channel currents were recorded (ACh in the pipette solution) from cells in a 35-mm dish with 1.8 ml ECS. Then, 0.2 ml of ECS containing a tenfold concentration of CBD was added to the dish to yield the final concentration required for each experiment. For inside-out patches, channels were recorded after excising the patch before and after CBD addition following the same strategy as described above.

For each condition, n indicates the number of recordings from different cell patches, and N, the number of cell transfections, each from different days and cell batches.

Measurement of changes in intracellular calcium levels ($[Ca^{2+}]_i$)

Cells expressing α7 nAChR were grown in cover-glass bottomed culture dishes (coated with poly-L-ornithine) in DMEM. Before the experiments, cells were preincubated with 1 μM atropine (antagonist of cholinergic muscarinic receptors). Atropine was maintained throughout the whole experiment. Cells were then loaded with 3 μM of the Ca^{2+}-sensitive fluorescent indicator fluo-3/AM for 30 min at room temperature in Fura Buffer (138 mM NaCl, 5 mM KCl, 1 mM $MgCl_2$, 5 mM glucose, 10 mM HEPES, 1.5 mM $CaCl_2$, 0.1% bovine serum albumin, pH 7.4). Cells were washed and incubated for 30 min with 1 mM probenecid in the same buffer.

$[Ca^{2+}]_i$ was measured using a confocal laser scanning microscope (LSM 900 Zeiss) with a 10× objective and 10× eyepiece. Fluo-3/AM-loaded cells were excited at 506 nm, and the fluorescence emission above 526 nm was recorded using the software Zen 3.0 Blue edition (Zeiss, Germany). Images of fluorescence were obtained at a rate

of one frame every 0.633 s during 180 s. 500 µM ACh and 3 µM PNU-120596 were added directly to the samples to elicit α7 nAChR activation. 10 µM CBD (in 1%v/v ethanol) or ethanol alone (1%v/v) was added to the cells 3 min before addition of 500 µM ACh and 3 µM PNU-120596. To determine specificity, cells were incubated with 1 µM α-bungarotoxin (α-BTX) before the addition of the fluo-3/AM and were included in solutions throughout the whole experiment. Analysis of the fluorescence was performed by Zen lite software.

Basal fluorescence (F_0) was determined prior to the addition of α7 nAChR ligands, and measurements were normalized to this F_0 value (F/F_0 ratio) for each condition. All conditions were measured in parallel assays, and the whole experiment was repeated with different batches of cells and transfections. For quantification, for each individual assay, we determined the values of F_0 (time 0) and F_{45} (45 s after the stimulus of 500 µM ACh and 3 µM PNU-120596) for a total of 10 to 25 cells in the same field, and the mean F_{45}/F_0 value was calculated. The resulting F_{45}/F_0 values of different assays for each condition were averaged, and the results were expressed as mean ± SD.

Statistical analysis

Data are presented as mean ± SD. Data sets were analyzed using the two-tailed Student's t-test or Mann–Whitney rank sum test for pairwise comparisons or one-way ANOVA for multiple comparisons with SigmaPlot 12.0 (Systat Software, Inc.). Statistically significant differences between two groups of data were established at p values < 0.05. Dose–response curves were fitted by a logistic function using SigmaPlot 12, from which IC_{50} (half inhibitory concentration) values were obtained and expressed as mean ± SEM.

Results

CBD modulates α7 nAChR single-channel activity

We explored the effects of CBD as an α7 nAChR modulator using high-resolution single-channel recordings. Control recordings with 100 µM ACh in the pipette solution showed that > 90% patches exhibited channel activity ($n = 38$, $N = 15$; Fig. 1). Channel activity appeared as brief and isolated openings ($\tau_{open} \sim 0.1$–0.3 ms) or less often as several openings in quick succession, known as bursts ($\tau_{burst} \sim 0.35$–0.50 ms). Each burst corresponds to the activation of a single receptor molecule (Fig. 1) [37, 38, 42, 43]. Although the frequency of channel activity (isolated openings and bursts) was variable among patches due to variations in receptor expression levels, recordings with 100 µM ACh and 50 µM CBD in the pipette solution showed systematically reduced channel

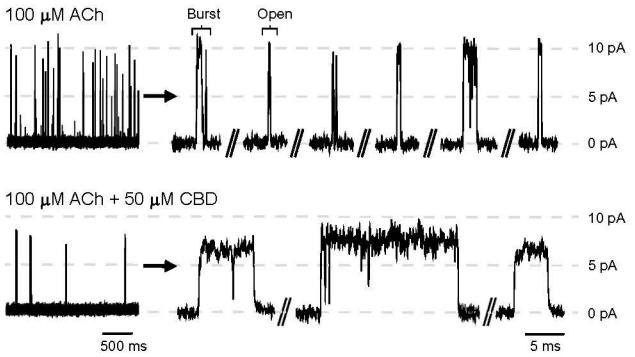

Fig. 1 Effects of CBD on single-channel currents of α7 nAChR elicited by ACh. Single-channel currents of α7 nAChR were recorded in the presence of 100 µM ACh with or without 50 µM CBD in the pipette solution. For each condition, representative channel traces are shown at two different temporal scales. Membrane potential: −70 mV. Filter: 9 kHz. Openings are shown as upward deflections

activity compared to control recordings performed in parallel ($n = 12$, $N = 4$) (Fig. 1). We also noted that after several minutes of recording prolonged bursts of slightly smaller amplitude appeared at a low frequency only in recordings in which CBD was present together with ACh (Fig. 1).

These observations suggested that CBD mediates at least two different actions, rapid inhibition of channel activity, followed by the appearance of prolonged openings and bursts with smaller amplitude than the typical α7 nAChR channels. Thus, we analyzed both phenomena using different strategies.

To quantify the reduction of the frequency of channel activity as a function of CBD concentration, we recorded single-channel currents elicited by 100 µM ACh present in the pipette solution. Then, ECS solution containing CBD was added to the dish to yield the required final concentration, and single channels were recorded again for the same period of time (Fig. 2). The advantage of this strategy is that it allows the comparison of the frequency of channel activity in the absence and presence of the drug in the same patch, and therefore, the measurements are not affected by the variability of receptor expression among different patches [38]. For determining the frequency of channel activity, we measured the number of bursts/min. We did not establish any limit in the number of openings to define a burst. Therefore, bursts include all activation episodes that occur either as isolated single openings or as bursts composed of several openings in quick succession separated by closings briefer than the critical duration.

As shown in Fig. 2A, CBD induced a marked concentration-dependent decrease in the frequency of channel opening. To quantify this effect, we measured for each patch the number of bursts/min before and in the interval of time between minute 2 and 10 after the addition of CBD

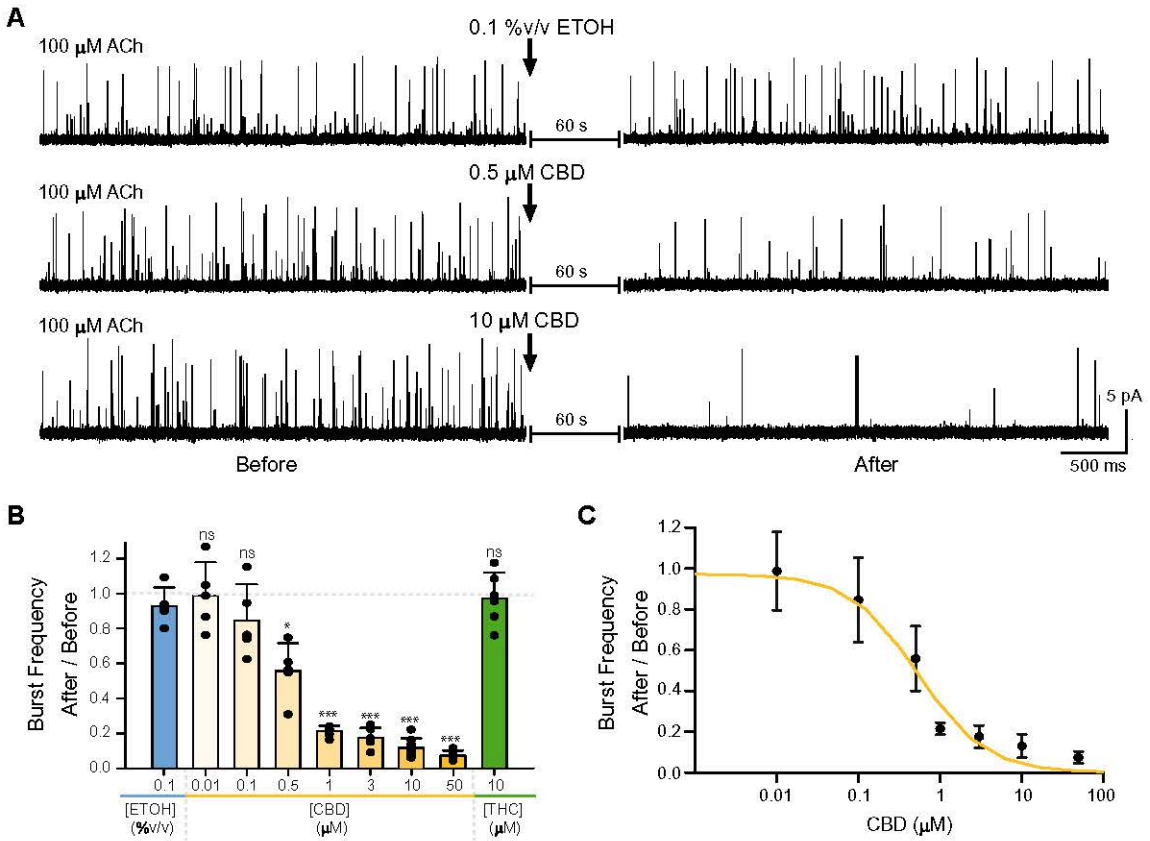

Fig. 2 CBD reduces channel activity in a concentration-dependent manner. Single-channel currents of α7 nAChR activated by 100 µM ACh were recorded in the cell-attached patch configuration (before), and 2 to 10 min after the addition to the dish of ethanol (0.1%v/v), CBD at different final concentrations or THC (10 µM) (after). The CBD concentration values correspond to the final concentrations in the ECS in contact with the cells. **A** Single-channel traces of typical recordings before and after exposure to 0.1%v/v ethanol, 0.5 µM CBD or 10 µM CBD. Channel openings are shown as upward deflections. Membrane potential: −70 mV. Filter 9 kHz. **B** Bar chart showing the change in the number of bursts/min due to the addition of ethanol, CBD at different concentrations, or 10 µM THC. For each recording, the number of bursts was measured during the same period of time before and after exposure to the drugs. The ratio of the number of bursts/min after/before drug exposure was calculated for each patch (individual data points). The mean ± SD of the ratios for $n=5$, $N=3$ (0.1%v/v ethanol); $n=5$, $N=3$ (0.01 µM CBD); $n=5$, $N=3$ (0.1 µM CBD); $n=5$, $N=2$ (0.5 µM CBD); $n=6$, $N=3$ (1 µM CBD); $n=6$, $N=2$ (3 µM CBD); $n=8$, $N=4$ (10 µM CBD); $n=5$, $N=3$ (50 µM CBD); and $n=6$, $N=2$ (10 µM THC) are shown. Statistical comparisons were performed by two-tailed Student's t test between ethanol and CBD or THC conditions (ns: not significant, $p \geq 0.05$; asterisk symbol (*) indicates statistical significance: $p<0.05$*; $p<0.01$**; $p<0.001$***). **C** Concentration–response curve for the inhibition of channel frequency, measured from the ratio of the number of bursts/min (after/before drug addition) as a function of the final CBD concentration. Each point corresponds to the mean of 5 to 8 independent experiments as described in **B**. Dose–response curves were fitted by a logistic function using SigmaPlot 12, from which IC_{50} (half maximal inhibitory concentration) value was obtained and expressed as mean ± SEM

or ethanol as the control (0.1%v/v final concentration). The ratios determined for each patch were averaged for different experiments. The addition of ethanol produced a very slight reduction in the frequency of bursts (ratio after/before = 0.93 ± 0.10; $n=5$, $N=3$), probably due to the expected desensitization of α7 nAChR (Fig. 2A, B). In contrast, a profound decrease in the frequency of channel activity occurred a few seconds after the addition of CBD. Figure 2B shows that the reduction of the frequency, measured by the ratio of bursts/min after/before CBD addition, was statistically significant at concentrations as low as 500 nM (ratio after/before = 0.56 ± 0.16; $n=5$, $N=2$; $p=0.00238$) and that 50 µM CBD led to a > 90% channel inhibition (ratio after/before = 0.07 ± 0.03; $n=5$, $N=3$; $p=0.000000112$). The fit to the data revealed that CBD inhibits α7 nAChR channel activity with an IC_{50} of 0.53 ± 0.14 µM (Fig. 2C).

To test reversibility of the decrease in burst frequency mediated by CBD (10 µM), we replaced three times the ECS to washout the free CBD. We found no significant reversion of burst frequency after 8 to 10 min of complete ECS exchange. The ratio of burst frequency observed after washout (burst frequency after washout/ before CBD addition) was 0.17 ± 0.05 ($n=3$, $N=2$). This ratio was similar to that determined in the presence of CBD (burst

frequency after CBD/before CBD addition: 0.15 ± 0.06; $n = 3$, $N = 2$; $p = 0.634$). The lack of reversibility may be due to the fact that CBD remains in the membrane due to its high hydrophobicity during the tested period or that it shows a slow unbinding time constant from the receptor [46].

To explore in detail the later appearance of longer duration activation episodes (openings or bursts) with reduced amplitude in the presence of CBD, we applied two different strategies from single-channel recordings, one including CBD in the pipette solution and the other adding CBD to the dish during the recording.

We first analyzed the recordings in which 50 μM CBD was included in the pipette solution together with 100 μM ACh as described in Fig. 1. For the control condition (100 μM ACh), open and burst duration histograms showed two exponential components and the mean duration of the slowest component was 0.30 ± 0.06 ms (τ_{open}) and 0.46 ± 0.12 ms (τ_{burst}), respectively ($n = 38$, $N = 15$; Fig. 3A, B). In the presence of 50 μM CBD, there was a 4.8-fold increase in the mean open duration ($\tau_{open} = 1.47 \pm 0.38$ ms; $n = 12$, $N = 4$; $p = 0.001$) and 5.1-fold increase in the mean burst duration ($\tau_{burst} = 2.36 \pm 0.54$ ms; $n = 12$, $N = 4$, $p = 0.001$) (Fig. 3A).

Control recordings of α7 nAChR activated by ACh showed a wide range of channel amplitudes because their brief open durations do not allow full resolution at our recording conditions [43]. However, if only events longer than 0.3 ms are considered, a homogenous amplitude class of 10.05 ± 0.15 pA was detected ($n = 5$, $N = 4$) [38, 43, 47]. In the presence of 50 μM CBD, amplitude histograms constructed for events longer than 0.3 ms showed a mean amplitude of 8.36 ± 0.24 pA ($n = 12$, $N = 4$), which was smaller than that of the control ($p = 0.00000386$) (Fig. 3A).

We also analyzed the duration of bursts from experiments in which different concentrations of CBD were added to the dish during the course of the recording as described in the experiments shown in Fig. 2. Besides the rapid reduction in channel activity, longer duration openings and bursts were clearly detected after several minutes (typically after about 10 min) of exposure to CBD concentrations higher than 1 μM. The mean open and burst durations of channels recorded after addition of 50 μM CBD were markedly longer than those determined in the same patch before its addition. This increase was about threefold for the mean open duration (τ_{open} before = 0.28 ± 0.04 ms and τ_{open} after = 0.89 ± 0.30 ms; $n = 5$, $N = 3$; $p = 0.00190$) and fivefold for the mean burst duration (τ_{burst} before = 0.44 ± 0.11 ms and τ_{burst} after = 2.25 ± 0.90 ms; $n = 5$, $N = 3$; $p = 0.00211$). Figure 3B shows the increase in burst duration (τ_{burst}), quantified by the ratio of τ_{burst} after and before drug addition, for different CBD concentrations. The increase was dependent on CBD concentration and was statistically significant at 1 μM CBD.

To determine if ethanol used as the vehicle for CBD was mediating the changes in channel properties, we recorded α7 nAChR channels in the presence of 100 μM ACh before and after addition of ethanol (0.1%v/v). The addition of ethanol did not produce changes in the mean open and burst durations (Fig. 3B). The values of τ_{open} were 0.24 ± 0.03 ms and 0.24 ± 0.05 ms before and after ethanol addition, respectively ($n = 5$, $N = 3$; $p = 0.796$); and τ_{burst} were 0.38 ± 0.07 ms and 0.36 ± 0.09 ms before and after ethanol addition, respectively ($n = 5$, $N = 3$; $p = 0.847$).

To confirm that the long-duration openings corresponded to α7 nAChR channels, we made recordings from non-transfected cells in the presence of 100 μM ACh. No channel openings were detected before or after addition of 50 μM CBD ($n = 5$, $N = 3$), thus indicating that the long openings arise from α7 nAChR activity.

The fraction of time that the channel is in the open state (nP_o) depends both on the frequency of channel opening and the duration of each opening. After short times of CBD exposure (less than 10 min), nPo decreased to a similar extent to the burst frequency, showing an IC_{50} value of 0.44 ± 0.15 μM.

Given the later appearance of long-duration openings and bursts, we explored at longer times of exposure how it affected nPo. We found that after longer times of exposure to 10 μM CBD, measured between minutes 15 and 18, the ratio of nPo increased with respect to the ratio measured between 2 and 5 min exposure (0.54 ± 0.21 and 0.15 ± 0.04, respectively; $n = 3$, $N = 3$; $p = 0.036$). In contrast, the burst frequency (after/ before CBD) remained similarly low at both periods (0.11 ± 0.02 and 0.12 ± 0.04, respectively; $n = 3$, $N = 3$; $p = 0.864$). The increase in nPo was therefore due to the appearance of the infrequent long-duration openings and bursts and not to an increase in channel frequency.

Taken together, our results revealed that CBD has dual actions at α7 nAChR, which consist in a rapid and marked decrease in channel activity, followed by partial recovery of the activity of channels with different kinetics and amplitude properties.

We tested if THC, which is the psychoactive component of marijuana, also affects α7 nAChR channel frequency. After recording single-channel activity elicited by ACh, 10 μM THC was added to the dish (final concentration), and the ratio of the frequency of bursts (after/before THC) was averaged for different patches. In contrast to the results with CBD, non-statistically significantly differences were observed on channel opening frequency after addition of THC (ratio after/before = 0.97 ± 0.15; $n = 6$; $N = 2$, $p = 0.971$) (Fig. 2B). Also, the mean open and burst durations remained unaffected after 10 min addition of THC (τ_{open} before = 0.25 ± 0.08 ms and τ_{open} after = 0.24 ± 0.07 ms; $n = 6$; $N = 2$; $p = 0.826$; τ_{burst} before = 0.40 ± 0.18 ms and τ_{burst} after = 0.42 ± 0.20 ms; $n = 6$; $N = 2$; $p = 0.937$) (Fig. 3B).

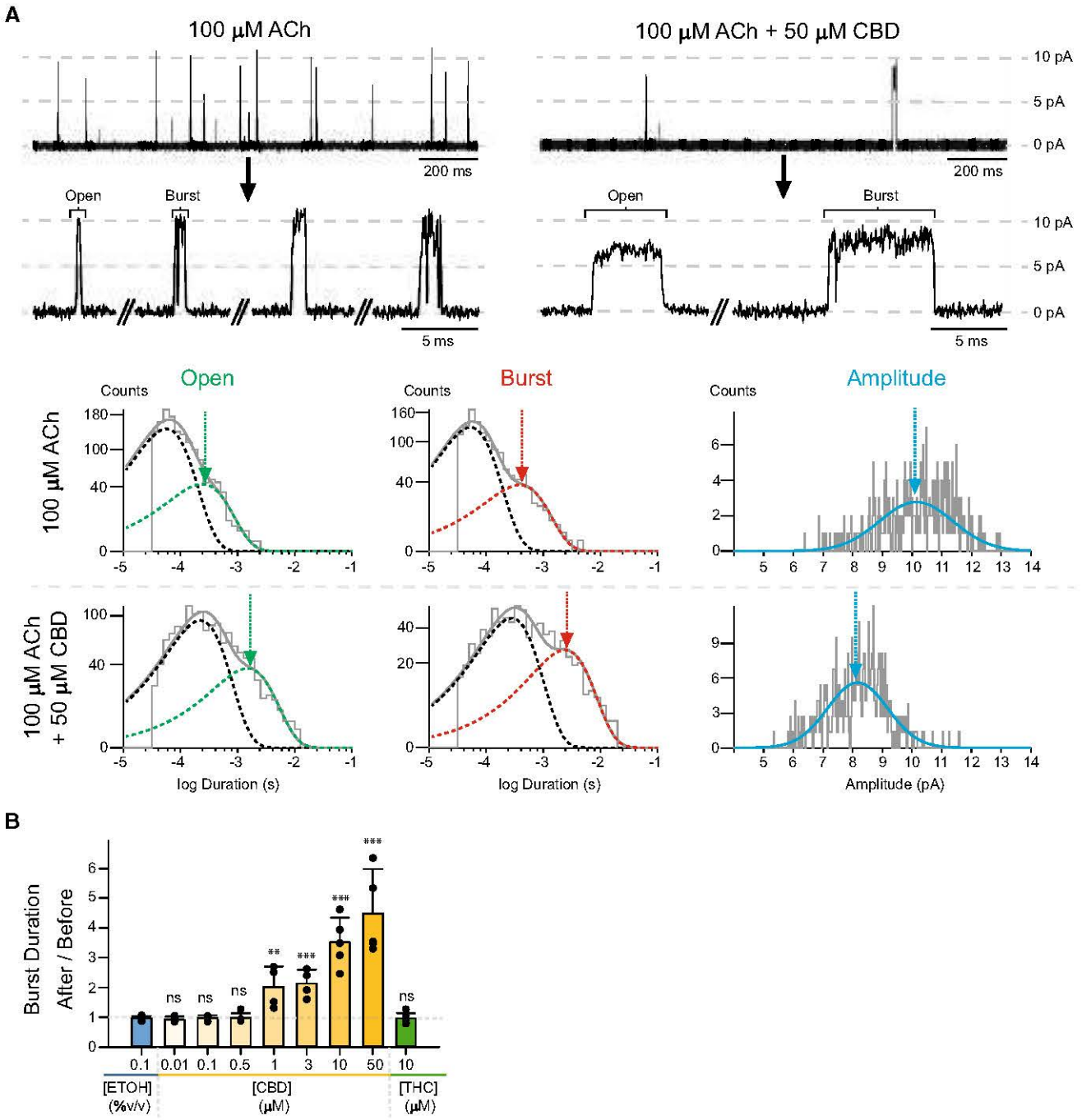

Fig. 3 Novel modulation of α7 nAChR by CBD revealed by different application strategies. **A** Single-channel currents were recorded in the presence of 100 µM ACh in the absence or presence of 50 µM CBD in the pipette solution. Top: Typical channel traces of α7 nAChR recording in the absence and presence of CBD are shown at two different temporal scales. Membrane potential: −70 mV. Filter: 9 kHz. Bottom: Representative histograms of open and burst durations and amplitude are shown. Amplitude histograms were constructed for events longer than 0.3 ms. The arrows indicate the duration of the slowest component for the dwell time histograms and the mean amplitude for the amplitude histogram. **B** Channels were recorded in the cell-attached patch before and after CBD addition to the dish (after about 10 min). Bar chart shows the change in mean burst duration (τ_{burst}) due to the addition of ethanol, CBD at different concentrations, or THC to the dish. The concentration values correspond to the final concentrations of the drugs in the ECS to which the cells were exposed during the recording. The ratio of the mean burst duration after/before drug addition was calculated for each patch. The bars show the values for independent experiments and the mean ± SD of the ratios for $n=5$, $N=3$ (0.1%v/v ethanol); $n=5$, $N=3$ (0.01 µM CBD); $n=4$, $N=2$ (0.1 µM CBD); $n=5$, $N=2$ (0.5 µM CBD); $n=4$, $N=3$ (1 µM CBD); $n=4$, $N=2$ (3 µM CBD); $n=5$, $N=3$ (10 µM CBD); $n=5$, $N=3$ (50 µM CBD); and $n=6$, $N=2$ (10 µM THC). Statistical comparisons were performed by two-tailed Student's t test between ethanol and CBD or THC conditions (ns: not significant, $p \geq 0.05$; asterisk symbol (*) indicates statistical significance: $p<0.05$*; $p<0.01$**; $p<0.001$***)

Effects of CBD on α7 nAChR channel frequency in the presence of PAMs

To further analyze the mechanism underlying the profound decrease in channel frequency, we determined if it also occurred in the presence of PAMs. To this end, single channels were recorded in the presence of 100 μM ACh and a type I (5-HI) or a type II (PNU-120596) PAM in the pipette solution.

ACh elicited activity was potentiated in the presence of 2 mM 5-HI, which was evidenced as prolonged openings and bursts composed of successive openings of about 4 ms as described before (Fig. 4A) [38, 45]. The addition of CBD to the dish produced a marked concentration-dependent decrease in channel activity. The reduction in the number of bursts/min was statistically significant at final CBD concentrations as low as 100 nM (ratio after/before = 0.67 ± 0.10; $n = 5$, $N = 3$; $p = 0.010$) with respect to ethanol alone (ratio after/before = 0.96 ± 0.16; $n = 5$, $N = 3$). At 1 μM CBD, channel activity almost disappeared, and the burst frequency was only 8% of that measured before addition of the drug (ratio after/before = 0.08 ± 0.06; $n = 5$, $N = 3$; $p = 0.0000031$) (Fig. 4A, B).

In the presence of 1 μM PNU-120596, a high-efficacy type II PAM, channel activity elicited by 100 μM ACh showed long episodes of high-frequency openings, named clusters, with a mean duration of about 1–3 s and amplitude of ~ 10 pA (− 70 mV). A cluster comprises successive prolonged openings separated by brief closings and corresponds to the activation episode of the same receptor that oscillates between open and closed states before reaching a stable non-conducting desensitized state [40, 42] (Fig. 4C). As shown in the figure, both non-potentiated (isolated openings) and potentiated (clusters) events appear in the same recording.

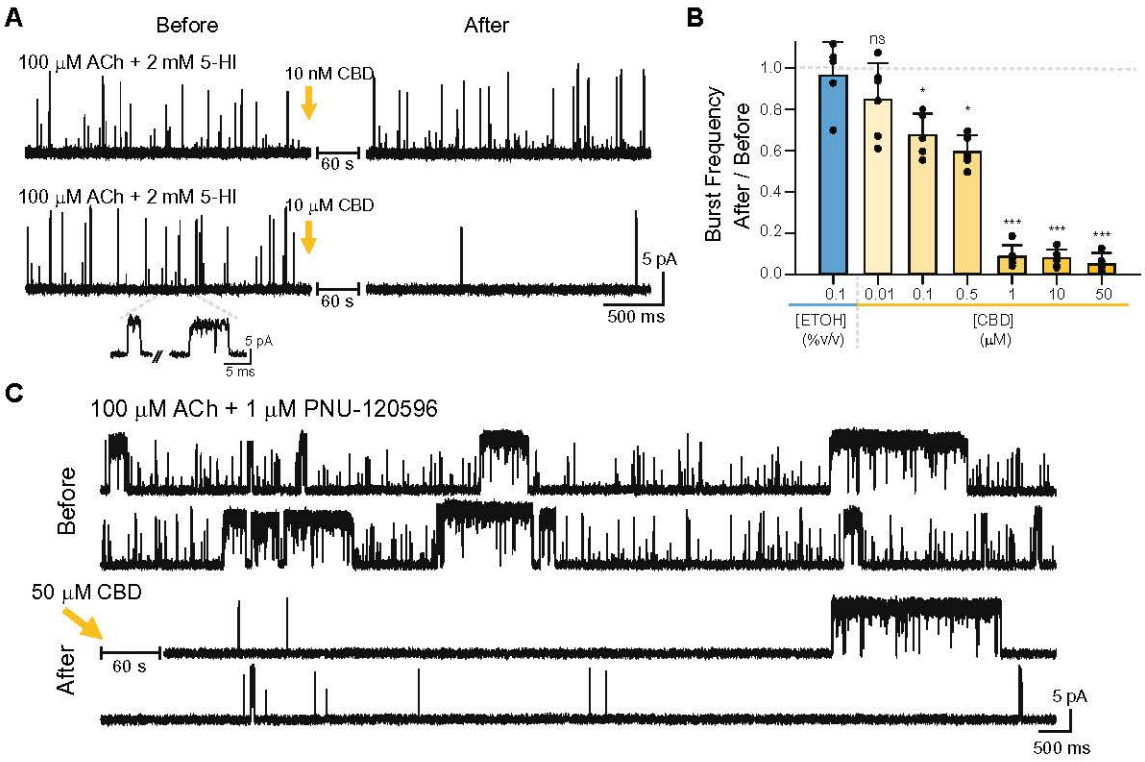

Fig. 4 CBD decreases frequency of α7 nAChR channels potentiated by type I and type II PAMs. **A** Recordings of α7 nAChR in the presence of 100 μM ACh and 2 mM 5-HI in the pipette solution. Typical channel traces recorded before and after addition of CBD (10 nM and 10 μM final concentrations) to the dish are shown (top). α7 nAChR channels potentiated by 5-HI are shown at a higher temporal resolution (bottom). Membrane potential: − 70 mV. Filter: 9 kHz. **B** Bar chart showing the reduction of burst frequency of α7 nAChRs activated by ACh and potentiated by 5-HI after addition of ethanol or CBD at different concentrations. For each recording, the number of bursts were measured during the same period of time before and after addition of the drugs. The ratio of the number of bursts/min after/before drug addition was calculated for each patch. The bars show the values for independent experiments and mean ± SD of the ratios for $n = 5$, $N = 3$ (0.1%v/v ethanol); $n = 6$, $N = 2$ (0.01 μM CBD); $n = 5$, $N = 3$ (0.1 μM CBD); $n = 5$, $N = 3$ (0.5 μM CBD); $n = 5$, $N = 3$ (1 μM CBD); $n = 5$, $N = 3$ (10 μM CBD); and $n = 5$, $N = 3$ (50 μM CBD). Statistical comparisons were performed by two-tailed Student's t-test between ethanol and CBD conditions (ns: not significant, $p \geq 0.05$; asterisk symbol (*) indicates statistical significance: $p < 0.05$*; $p < 0.01$**; $p < 0.001$***). **C** Single-channel traces of a continuous recording in the presence of 100 μM ACh and 1 μM PNU-120596 in the pipette solution before and after addition of CBD (50 μM final concentration). Membrane potential: -70 mV. Filter: 3 kHz

Channel activity was quantified by the number of clusters/min. However, clusters included all activation episodes that can occur as isolated openings or as the typical long-duration clusters since we did not establish any limit in the number of openings to consider a cluster. Addition of 50 μM CBD produced a statistically significant, ~ 90%, reduction in cluster frequency (ratio after/before = 0.10 ± 0.06; $n = 5$, $N = 3$; $p = 0.000000089$) compared to that of the control condition (ratio after/before = 0.96 ± 0.09; $n = 5$, $N = 3$) (Fig. 4C). Thus, CBD acts as a negative modulator in the presence of type I and type II PAMs.

Exploring structural basis underlying α7 nAChR modulation by CBD

To better understand the molecular basis of α7 nAChR modulation by CBD, we tested its inhibitory effect on mutant receptors. In this set of experiments, we compared the frequency of bursts before and after exposure to 3 μM CBD (final concentration). At this concentration, the reduction in burst frequency for the wild-type receptor was 82 ± 6% (ratio after/before = 0.18 ± 0.06; $n = 6$, $N = 2$) (Fig. 2B, Fig. 5).

To explore if CBD modulates α7 nAChR by affecting its phosphorylated state, we examined a double tyrosine mutant receptor (α7-Y386F/Y442F). This mutant receptor, which lacks the two tyrosine residues of the ICD, shows longer duration bursts, reduced desensitization rate and significantly faster recovery from desensitization than wild-type receptors [38]. After addition of 3 μM CBD to the dish, channel activity markedly decreased, leading to a reduction in the number of bursts/min of 75 ± 13% (ratio after/before = 0.25 ± 0.13; $n = 6$, $N = 3$) (Fig. 5). Thus, tyrosine phosphorylation of the ICD is not involved in CBD negative modulatory effects.

We also examined if serine/threonine phosphorylation was involved in CBD effects on α7 nAChR. We mutated to alanine, residues S365 and T331 of the ICD, that have the potential to be phosphorylated by serine/threonine protein kinases. As these mutant receptors have not been previously described, we first characterized their channel properties. The mean open and burst durations for channels activated by 100 μM ACh were 0.29 ± 0.03 ms and 0.42 ± 0.09 ms, respectively (α7-S365A, $n = 6$, $N = 3$); and 0.30 ± 0.08 ms and 0.46 ± 0.13 ms, respectively (α7-T331A, $n = 6$, $N = 3$). Thus, the mutations did not affect the kinetics of the receptor with respect to that of wild-type α7 nAChR (α7-S365A: $p = 0.620$ and $p = 0.383$ for τ_{open} and τ_{burst}, respectively; and α7-T331A: $p = 0.742$ and $p = 0.985$ for τ_{open} and τ_{burst}, respectively). Addition of 3 μM CBD during the course of the recording, also produced a profound decrease in the number of bursts/min of the mutants: 69 ± 11% for α7-S365A (ratio after/before = 0.31 ± 0.11; $n = 5$, $N = 3$) and 73 ± 17% for α7-T331A (ratio after/before = 0.27 ± 0.17; $n = 6$, $N = 3$)

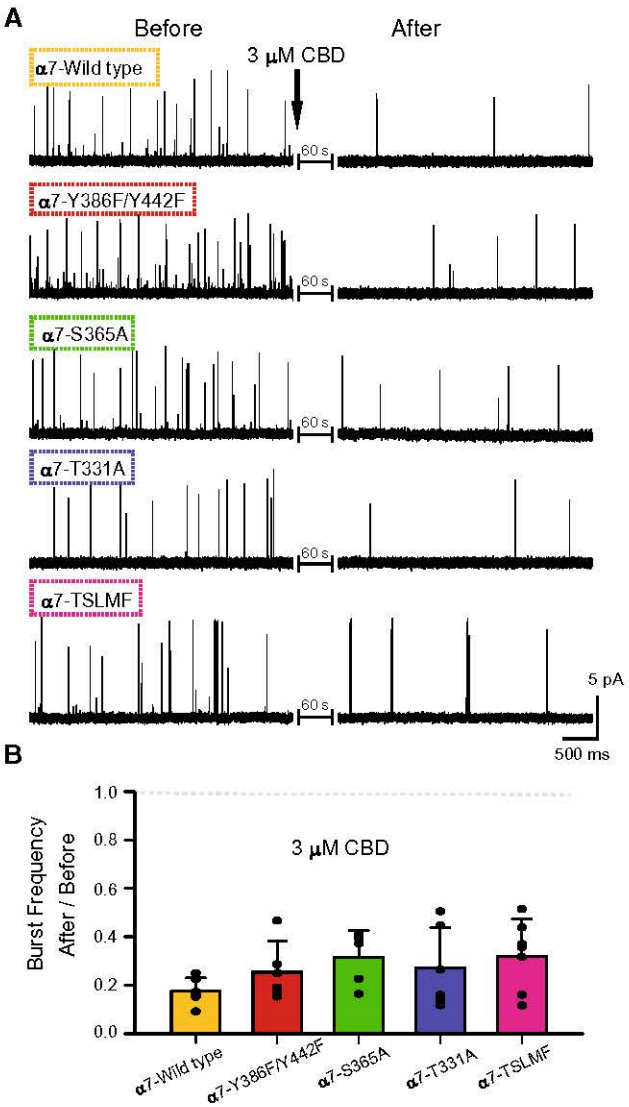

Fig. 5 CBD effects on mutant α7 nAChRs. **A** Typical channel traces from recordings of different α7 nAChR mutants activated by 100 μM ACh before and after addition of 3 μM CBD to the dish (final concentration) during the course of the recording. Membrane potential: −70 mV. Filter: 9 kHz. **B** Bar chart comparing the reduction of burst frequency due to exposure to 3 μM CBD among different α7 nAChR mutants. For each recording, the number of bursts was measured during the same period of time before and after addition of CBD. The ratio of the number of bursts/min after/before CBD addition was calculated for each patch. The bars show the values from independent experiments and mean ± SD of the ratios for $n = 6$, $N = 2$ (α7-wild-type); $n = 6$, $N = 3$ (α7-Y386F/Y442F); $n = 5$, $N = 3$ (α7-S365A); $n = 6$, $N = 3$ (α7-T331A); and $n = 7$, $N = 3$ (α7-TSLMF). Statistical comparisons among groups were performed by one-way ANOVA. The mean values among groups are not statistically significantly different ($p = 0.335$)

(Fig. 5). Thus, serine/threonine phosphorylation of these residues is not involved in CBD negative modulatory effects.

Previous studies have shown that simultaneous mutations of five transmembrane residues in α7 nAChR (α7-TSLMF)

inhibit potentiation by PNU-120596 and other PAMs, indicating that these residues are determinants for allosteric modulation [39–41]. This mutant receptor showed prolonged open ($\tau_{open} = 1.36 \pm 0.50$ ms; $n = 5$, $N = 3$; $p < 0.001$) and burst durations ($\tau_{burst} = 2.31 \pm 0.98$ ms; $n = 5$, $N = 3$; $p < 0.001$) with respect to wild-type α7 nAChR [40, 41]. Exposure to 3 μM CBD produced a profound reduction of the frequency of bursts: $68 \pm 15\%$ (ratio after/before $= 0.32 \pm 0.15$; $n = 7$, $N = 3$) (Fig. 5). Thus, determinants that affect PNU-120596 potentiation do not alter CBD inhibition of α7 nAChR.

Once established that all the analyzed mutants were inhibited by CBD, we explored if they showed differences in the degree of inhibition of channel activity. Comparison of the reduction of bursts/min after CBD addition among wild-type and mutant receptors showed no statistically significant differences in this parameter (one-way ANOVA test, $p = 0.335$), indicating similar sensitivity to CBD among wild-type and mutant α7 nAChRs (Fig. 5B).

Application of CBD to inside-out patches

To gain further insights into the basis of CBD action, we recorded single-channel currents activated by 100 μM ACh in the inside-out patch configuration, which allows bath perfusion of the cytoplasmic face of the membrane (Fig. 6). Channels were recorded from the excised patch before and after addition to the dish of ECS containing CBD to yield a final concentration of 50 μM. The exposure to CBD led to a profound, > 90%, channel frequency reduction (ratio after/before $= 0.07 \pm 0.05$; $n = 6$, $N = 2$). This value was similar to that obtained in the cell-attached configuration at the same concentration (ratio after/before $= 0.07 \pm 0.03$; $n = 5$, $N = 3$; $p = 0.662$). Moreover, the long-duration openings also appeared after several minutes of CBD exposure. We confirmed that CBD similarly affects α7 nAChR function from both sides of the membrane, thus indicating that it reaches its binding site in the receptor through a membrane pathway.

CBD inhibits agonist-elicited intracellular calcium mobilization

α7 nAChR activation triggers the increase in intracellular Ca^{2+} levels ($[Ca^{2+}]_i$). It has been shown that activation by the agonist in the presence of PNU-120596 induces larger and sustained calcium responses than by the agonist alone [45, 48–51]. To explore how CBD affects calcium mobilization elicited by α7 nAChR, we conducted confocal microscopy analysis of α7-expressing cells loaded with Fluo-3/AM. Receptors were activated by a pulse of 500 μM ACh together with 3 μM PNU-120596. Application of ACh and the PAM led to a rapid increase of $[Ca^{2+}]_i$, which was maintained during at least 3 min as shown in Fig. 7A.

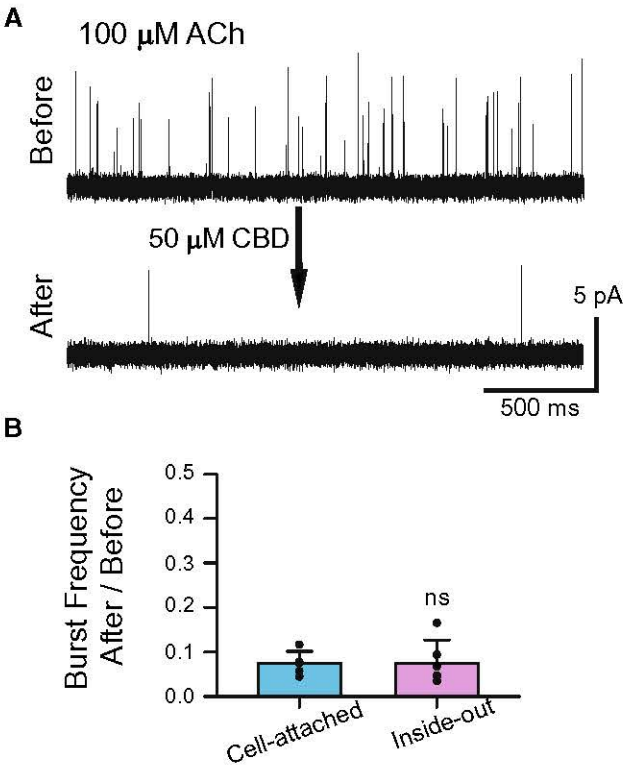

Fig. 6 Effect of CBD on α7 nAChR from the intracellular membrane side. **A** Typical channel traces from single α7 nAChR channel currents activated by 100 μM ACh recorded in the inside-out patch configuration before (top) and after addition of 50 μM CBD to the dish (final concentration). Membrane potential: −70 mV. Filter: 9 kHz. **B** Bar chart comparing the reduction of burst frequency due to 10 μM CBD between recordings in the cell-attached patch and inside-out patch configurations. The bars show the values from independent experiments and the mean ± SD of the ratio for $n = 5$, $N = 3$ (cell-attached patch) and $n = 6$, $N = 2$ (inside-out patch)

To quantify the change, we determined the F_{45}/F_0 ratio from fluorescence measurements before and 45 s after α7 nAChR activation by ACh and PNU-120596 as explained in Methods (Fig. 7). The increase in $[Ca^{2+}]_i$ induced by 500 μM ACh and 3 μM PNU-120596 ($F_{45}/F_0 = 5.6 \pm 0.7$; $n = 3$; $N = 1$) was not affected by a 3-min preincubation of cells with 1%v/v ethanol, which was the vehicle used for CBD ($F_{45}/F_0 = 5.7 \pm 2.3$; $n = 6$, $N = 3$; $p = 0.96$) (Fig. 7). In contrast, a profound reduction in the response to ACh and PNU-120596 was detected if cells were preincubated 3 min with 10 μM CBD ($F_{45}/F_0 = 2.0 \pm 0.7$; $n = 9$, $N = 4$; $p = 0.003$) (Fig. 7). No changes in intracellular calcium levels were detected in cells expressing α7 nAChR but preincubated during 3 h with the irreversible antagonist α-BTX (1 μM) ($F_{45}/F_0 = 1.0 \pm 0.1$; $n = 8$, $N = 4$; $p < 0.001$), indicating that the calcium increase was mediated by α7 nAChR. This set of experiments demonstrate that CBD mediates a profound decrease in cell calcium responses triggered by α7 nAChR activation.

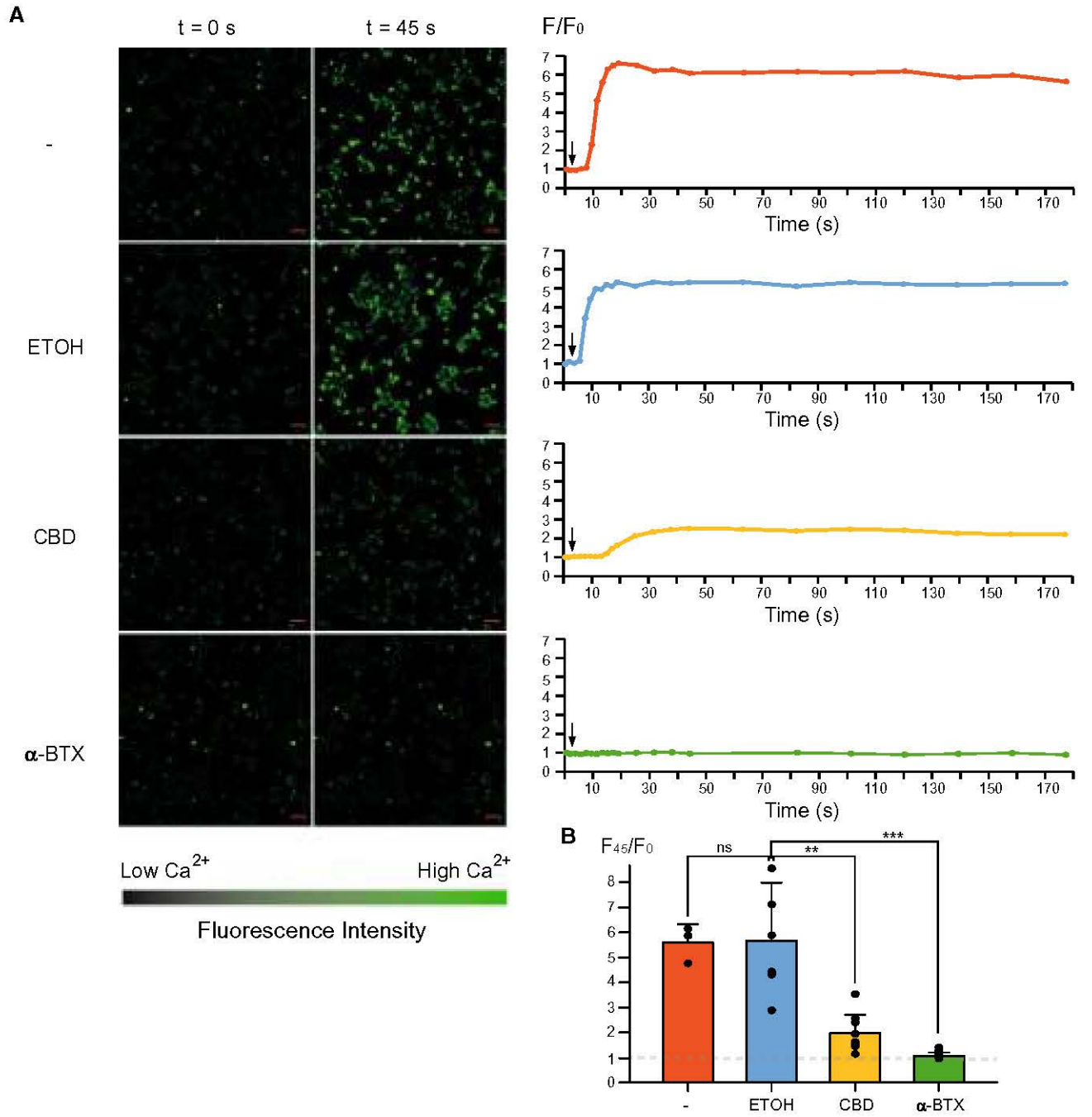

Fig. 7 Effects of CBD on intracellular calcium mobilization triggered by α7 nAChR. BOSC-23 cells expressing α7 nAChR were loaded with Fluo-3/AM, and analyzed by laser scanning confocal microscopy as described under Methods. The images were obtained immediately before (0 s) and after 45 s (45 s) of a pulse of 500 μM ACh and 3 μM PNU-120596 to activate the receptor. **A** Left: Confocal microscope images of cells. The scale corresponds to 50 μm and the total magnification was 100x. The different conditions correspond to different treatments before the ACh/PNU-120596 stimulus: ETOH: 3 min-preincubation with 1%v/v ethanol; CBD: 3 min-preincubation with 10 μM CBD in 1%v/v ethanol; α-BTX: 3 h-preincubation with 1 μM α-BTX and 3 min-preincubation with 1%v/v ethanol. The color scale represents the relative fluorescence intensity of Fluo-3/AM-loaded cells, with black representing the lowest and green the highest $[Ca^{2+}]_i$ levels. Right: typical curves for a given cell for each condition showing the changes in the relative fluorescence values calculated as F/F_0 as a function of time. The arrow indicates the time of ACh/PNU-120596 application. **B** Bars show values corresponding to independent experiments with about 10–25 cells in each assay (see Methods) and the mean ± SD of the F_{45}/F_0 ratio. ns: not significant, $p \geq 0.05$; asterisk symbol (*) indicates statistical significance: $p < 0.05$*; $p < 0.01$**; $p < 0.001$***

Discussion

CBD is emerging as a therapeutic agent for several pathological conditions due to a large body of evidence showing its therapeutic benefits and no psychoactive effects. CBD shows low affinity for cannabinoid receptors (CB1 and CB2) and acts as a pleiotropic drug by targeting a great variety of receptors, channels and signaling pathways [12]. We here reveal how CBD affects α7 nAChR ionotropic and metabotropic functions. It produces a profound concentration-dependent decrease in single-channel activity with an IC_{50} in the sub-micromolar range, indicating a potent negative modulation of pharmacological significance. However, CBD modulation is complex since, after channel activity inhibition, it leads to the later appearance of infrequent ACh-elicited α7 nAChR openings with different kinetics and amplitudes to the typical ones. At the cellular level, CBD negatively modulates α7 nAChR metabotropic function, which is revealed by a profound decrease of cell calcium responses triggered by α7 nAChR activation.

A few studies have shown that some endocannabinoids allosterically inhibit macroscopic responses of α7 nAChR expressed in oocytes [23, 24]. To our knowledge, there is only one report of CBD effects on α7 nAChR, showing that preincubation with CBD inhibits agonist-elicited currents in oocytes and rat hippocampal slices [25]. However, macroscopic current recordings cannot provide precise mechanistic information. By applying high-resolution single-channel recordings, we showed that CBD produces rapid and profound decrease in the frequency of activation episodes. The IC_{50} estimated for the channel activity inhibition (~ 0.5 μM) is significantly lower than that estimated previously from the reduction of the macroscopic currents (~ 11 μM, [25]), probably due to the higher temporal resolution of our measurements [52]. The decrease in the frequency of the activation episodes (both isolated openings and bursts) may be due to impaired channel opening, channel blockade, or stabilization of a desensitized state, all of which are manifested as reduced channel activity. We discard open-channel blockade since there was no concentration-dependent decrease in open channel lifetime [53]. Enhancement of desensitization has been suggested as a potential mechanism for the decrease in 5-HT_3A currents mediated by CBD [54]. In α7 nAChR, enhancement of the rate of desensitization results in decreased open durations since this rate governs open channel lifetime [37], an effect that was not detected. As a potent type II PAM, PNU-120596 decreases desensitization and recovers receptors from desensitized states [39, 41, 55]. Nevertheless, this PAM cannot overcome CBD inhibition, indicating that either CBD does not affect α7 nAChR desensitization or that it stabilizes a desensitized state that cannot be recovered by PNU-120596 [56]. Thus, it is likely that CBD inhibits α7 nAChR activity by impairing channel opening through stabilization of the closed resting state and/or stabilization of a PNU-120596-insensitive desensitized state (Fig. 8). Interestingly, CBD also shows state-dependence selectivity for voltage-gated sodium channels as it prevents activation from resting state and stabilizes the inactivated state [46, 57, 58].

The appearance of the longer openings and bursts with slightly reduced amplitude after CBD treatment attracted our attention as a novel modulatory process. Both ACh and CBD acting through α7 nAChR are required to generate this unique type of channel openings. The fact that the appearance of the atypical openings is a delayed effect with respect to the reduction in channel frequency suggests that these events may arise from CBD-bound channels that reopen from a CBD-stabilized conformational state (resting or desensitized) (Fig. 8). Alternatively, CBD may act through two different sites, one mediating the decrease of channel activity and the other, the changes in channel kinetics.

THC neither decreases α7 nAChR channel frequency nor changes open and burst durations. However, THC is active at other Cys-loop receptors, including glycine, 5-HT_3 and $GABA_A$ receptors [16, 18, 20–22]. CBD and THC share chemical structures, with the difference of the closure of a ring on THC as opposed to a free hydroxyl group in CBD.

To explore possible determinants of the CBD inhibitory action, we tested its effects on α7 nAChR mutants. We first evaluated if CBD reduces channel frequency by increasing receptor phosphorylation, which may take place indirectly by affecting intracellular signaling pathways that change kinase or phosphatase activities [59, 60]. We have previously shown that α7 nAChR tyrosine phosphorylation increases desensitization and decreases recovery rate from desensitization, resulting in reduced channel activity [38]. The α7 nAChR double mutant lacking tyrosine residues at the ICD (α7-Y386F/Y442F) also shows a marked decrease in channel

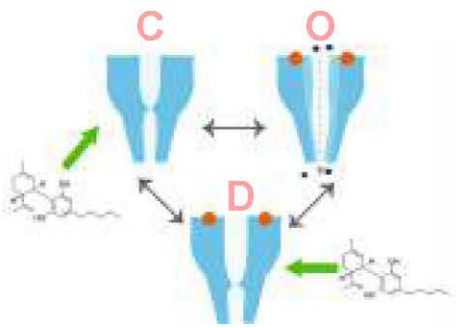

Fig. 8 Scheme for CBD mechanism of modulation. The scheme shows the main classes of conformational states: closed (C), open (O), and desensitized (D). The green arrows show the states that could be stabilized by CBD

activity in the presence of CBD, thus discarding enhanced tyrosine phosphorylation as a cause of CBD inhibition. We also tested if serine/threonine phosphorylation of α7 nAChR is involved in CBD action. By using NetPhos-3.1 server, we selected serine and threonine residues at the ICD that may have the potential of being phosphorylated. Previously, it was reported that S365 is phosphorylated by PKA [61]. Our first single-channel characterization of α7-T331A and α7-S365A mutants shows no changes in channel amplitude or in mean open and burst durations. The mutant receptors not only activate similarly to wild-type receptors, but they are similarly inhibited by CBD. Thus, neither tyrosine nor serine/threonine phosphorylation is involved in CBD inhibition of α7 nAChR activity.

CBD also inhibits the activity of the quintuple mutant α7-TSLMF receptor carrying mutations in residues located in M1, M2 and M3 transmembrane helices, which confer resistance to potentiation by PNU-120596 and other PAMs [40, 41]. Moreover, CBD is also capable of inhibiting α7 nAChR potentiated by type I or type II PAMs, indicating no competition with their actions.

Our results demonstrate that CBD reaches it binding site(s) through a membrane pathway, as also shown for CBD binding at voltage-gated sodium channels [46, 62]. Structural, mutagenesis, and computational studies have shown that a variety of hydrophobic allosteric ligands bind at different transmembrane sites of α7 nAChR and Cys-loop receptors [39, 63, 64]. The α7 nAChR structure in complex with PNU-120596 revealed that the PAM binds to a transmembrane cavity formed by transmembrane helices of adjacent subunits [65]. Thus, CBD may modify α7 nAChR activation by binding to one or more transmembrane sites, which remain to be defined. In addition, CBD has been shown to localize below the phosphate headgroups in bio-membranes and to increase the membrane stiffness [57]. As described for voltage-gated sodium channels [57], the changes in the biophysical properties of the membrane may also alter α7 nAChR activation properties, resulting in a complementary mechanism of CBD modulation. High-resolution structures of α7 nAChR in complex with CBD are required for precisely identify its binding site(s) which, in turn, could provide further insights into its molecular mechanisms, as well as for elucidating structural basis of cannabinoid selectivity.

α7 nAChR acts as a dual ionotropic-metabotropic receptor. Its activation triggers the opening of the cation-permeable channel, which results in rapid membrane depolarization and calcium influx into the cell. However, this fast ionotropic response is converted into a sustained, wide-ranging phenomenon by calcium release from intracellular stores through a calcium-induced calcium release mechanism, a process involving IP3 and ryanodine receptors [14, 27, 66, 67]. The increase in intracellular calcium levels has been shown to be associated with neuroprotection and inflammation [14, 33, 34] In our α7 nAChR-expressing cells, an increase in intracellular calcium was clearly detected after stimulation with ACh in the presence of PNU-120596, and was abolished by α-BTX, confirming that it was mediated by α7 nAChR. The precise mechanism that couples ionotropic to metabotropic activities, including calcium mobilization from intracellular stores, still remains unclear and may differ among different types of cells [27]. Nevertheless, our results show that the rapid cell calcium response mediated by α7 activation is significantly reduced after a very brief pre-exposure to CBD.

CBD modulation of Cys-loop receptors has pharmacological relevance. In this regard, CBD inhibition of 5-HT_3 receptors may contribute to its role in modulation of nociception and emesis, potentiation of GABA receptors may account for its anti-seizure, anxiolytic and analgesic effects, and potentiation of glycine receptors may be relevant for CBD anti-nociceptive actions [3, 16, 22]. Potentiation of α7 nAChR is required for improving cognition and memory and has neuroprotective, anti-nociceptive, and anti-inflammatory effects [14, 33, 34]. On the other hand, α7 nAChR mediates oncogenic signal transduction during cancer development, promotes cancer cell proliferation and metastasis in lung, gastrointestinal, and bladder tissues [35, 68]. Therefore, α7 nAChR inhibition has been proposed as a potential therapeutic strategy for several types of cancer associated with overexpressed α7 [68, 69]. For these pathological situations, CBD acting through α7 nAChR could be therapeutically beneficial.

The concentration range at which CBD modulates α7 nAChR is similar to that at which it is active on other channels, transporters, and receptors, including Cys-loop receptors [22, 54, 70–72]. Commonly used CBD doses in animal models resulted in mean plasma CBD levels in the low micromolar range [71, 73, 74], although its membrane concentration is expected to be higher than blood levels. Therefore, the functional modulation of α7 nAChR by CBD may be of pharmacological relevance and should be considered in the evaluation of prospective therapeutic uses. Due to the CBD promiscuous pharmacological activities, some may contribute to beneficial effects, others to adverse effects, and others may counteract effects of other therapeutic drugs under different pathological conditions [71]. Thus, as the interest in CBD as a therapeutic drug for a vast repertoire of health conditions increases and the CBD product industry shows increasing growth, molecular information related to CBD multiple actions and targets acquires great significance by providing the basis for understanding its applications in human health.

Acknowledgements We thank Drs. Fernando J. Sepulveda and Gonzalo Yevenes (Universidad de Concepción, Chile) for kindly providing CBD, Dr. Susana Pasquaré (Instituto de Investigaciones Bioquímicas

de Bahía Blanca, CONICET) for providing THC, and Mrs Carolina Paladino for technical contributions.

Author contributions JFC, MCE and CB designed and performed the research, analyzed the data and wrote, reviewed and edited the paper; CB supervised the study.

Funding This work was supported by grants from Universidad Nacional del Sur (PGI 24/B298 to CB and PGI 24/ZB79 to MCE), Agencia Nacional de Promoción Científica y Tecnológica PICT 2017-1170 and PICT 2020-00936 to CB), Consejo Nacional de Investigaciones Científicas y Técnicas (CONICET) PIP11220200102356.

Availability of data and material The data that support the findings of this study are available within the article.

Code availability Not applicable.

Declarations

Conflict of interest The authors report no conflict of interest.

Ethics approval and consent to participate Not applicable.

Consent for publication Not applicable.

References

1. Friedman D, Devinsky O (2015) Cannabinoids in the treatment of epilepsy. N Engl J Med 373:1048–1058. https://doi.org/10.1056/NEJMRA1407304
2. Russo EB, Guy GW, Robson PJ (2007) Cannabis, pain, and sleep: Lessons from therapeutic clinical trials of sativexρ, a cannabis-based medicine. Chem Biodivers 4:1729–1743
3. Vitale RM, Iannotti FA, Amodeo P (2021) The (poly)pharmacology of cannabidiol in neurological and neuropsychiatric disorders: molecular mechanisms and targets. Int J Mol Sci 22:4876. https://doi.org/10.3390/IJMS22094876
4. Soderstrom K, Soliman E, van Dross R (2017) Cannabinoids modulate neuronal activity and cancer by CB1 and CB2 receptor-independent mechanisms. Front Pharmacol. https://doi.org/10.3389/FPHAR.2017.00720
5. Izzo AA, Borrelli F, Capasso R et al (2009) Non-psychotropic plant cannabinoids: new therapeutic opportunities from an ancient herb. Trends Pharmacol Sci 30:515–527. https://doi.org/10.1016/J.TIPS.2009.07.006
6. Pertwee R (2010) Receptors and channels targeted by synthetic cannabinoid receptor agonists and antagonists. Curr Med Chem 17:1360–1381. https://doi.org/10.2174/092986710790980050
7. Hill AJ, Williams CM, Whalley BJ, Stephens GJ (2012) Phytocannabinoids as novel therapeutic agents in CNS disorders. Pharmacol Ther 133:79–97. https://doi.org/10.1016/J.PHARMTHERA.2011.09.002
8. Abu-Sawwa R, Scutt B, Park Y (2020) Emerging use of epidiolex (Cannabidiol) in epilepsy. J Pediatr Pharmacol Ther 25:485–499. https://doi.org/10.5863/1551-6776-25.6.485
9. Arzimanoglou A, Brandl U, Cross JH et al (2020) Epilepsy and cannabidiol: a guide to treatment. Epileptic Disord 22:1–14. https://doi.org/10.1684/EPD.2020.1141
10. Ibeas Bih C, Chen T, Nunn AVW et al (2015) Molecular targets of cannabidiol in neurological disorders. Neurotherapeutics 12:699–730. https://doi.org/10.1007/S13311-015-0377-3
11. McPartland JM, Duncan M, di Marzo V, Pertwee RG (2015) Are cannabidiol and Δ(9) -tetrahydrocannabivarin negative modulators of the endocannabinoid system? A systematic review. Br J Pharmacol 172:737–753. https://doi.org/10.1111/BPH.12944
12. de Almeida DL, Devi LA (2020) Diversity of molecular targets and signaling pathways for CBD. Pharmacol Res Perspect. https://doi.org/10.1002/PRP2.682
13. Peng J, Fan M, An C et al (2022) A narrative review of molecular mechanism and therapeutic effect of cannabidiol (CBD). Basic Clin Pharmacol Toxicol 130:439–456. https://doi.org/10.1111/BCPT.13710
14. Bouzat C, Lasala M, Nielsen BE et al (2018) Molecular function of α7 nicotinic receptors as drug targets. J Physiol 596:1847–1861. https://doi.org/10.1113/JP275101
15. Yang Z, Aubrey KR, Alroy I et al (2008) Subunit-specific modulation of glycine receptors by cannabinoids and N-arachidonylglycine. Biochem Pharmacol 76:1014–1023. https://doi.org/10.1016/J.BCP.2008.07.037
16. Xiong W, Wu X, Lovinger DM, Zhang L (2012) A common molecular basis for exogenous and endogenous cannabinoid potentiation of glycine receptors. J Neurosci 32:5200–5208. https://doi.org/10.1523/JNEUROSCI.6347-11.2012
17. Yévenes GE, Zeilhofer HU (2011) Molecular sites for the positive allosteric modulation of glycine receptors by endocannabinoids. PLoS ONE. https://doi.org/10.1371/JOURNAL.PONE.0023886
18. Xiong W, Cheng K, Cui T et al (2011) Cannabinoid potentiation of glycine receptors contributes to cannabis-induced analgesia. Nat Chem Biol 7:296–303. https://doi.org/10.1038/NCHEMBIO.552
19. Barann M, Molderings G, Brüss M et al (2002) Direct inhibition by cannabinoids of human 5-HT3A receptors: probable involvement of an allosteric modulatory site. Br J Pharmacol 137:589–596. https://doi.org/10.1038/SJ.BJP.0704829
20. Xiong W, Koo BN, Morton R, Zhang L (2011) Psychotropic and nonpsychotropic cannabis derivatives inhibit human 5-HT(3A) receptors through a receptor desensitization-dependent mechanism. Neuroscience 184:28–37. https://doi.org/10.1016/J.NEUROSCIENCE.2011.03.066
21. Sigel E, Baur R, Rácz I et al (2011) The major central endocannabinoid directly acts at GABA(A) receptors. Proc Natl Acad Sci USA 108:18150–18155. https://doi.org/10.1073/PNAS.1113444108
22. Bakas T, van Nieuwenhuijzen PS, Devenish SO et al (2017) The direct actions of cannabidiol and 2-arachidonoyl glycerol at GABA A receptors. Pharmacol Res 119:358–370. https://doi.org/10.1016/J.PHRS.2017.02.022
23. Oz M, Ravindran A, Diaz-Ruiz O et al (2003) The endogenous cannabinoid anandamide inhibits alpha7 nicotinic acetylcholine receptor-mediated responses in Xenopus oocytes. J Pharmacol Exp Ther 306:1003–1010. https://doi.org/10.1124/JPET.103.049981
24. Oz M, Zhang L, Ravindran A et al (2004) Differential effects of endogenous and synthetic cannabinoids on alpha7-nicotinic acetylcholine receptor-mediated responses in Xenopus Oocytes. J Pharmacol Exp Ther 310:1152–1160. https://doi.org/10.1124/JPET.104.067751
25. Mahgoub M, Keun-Hang SY, Sydorenko V et al (2013) Effects of cannabidiol on the function of α7-nicotinic acetylcholine receptors. Eur J Pharmacol 720:310–319. https://doi.org/10.1016/J.EJPHAR.2013.10.011
26. Egea J, Buendia I, Parada E et al (2015) Anti-inflammatory role of microglial alpha7 nAChRs and its role in neuroprotection. Biochem Pharmacol 97:463–472
27. Kabbani N, Nichols RA (2018) Beyond the channel: metabotropic signaling by nicotinic receptors. Trends Pharmacol Sci 39:354–366

28. Albuquerque EX, Pereira EFR, Alkondon M, Rogers SW (2009) Mammalian nicotinic acetylcholine receptors: from structure to function. Physiol Rev 89:73–120
29. Dickinson JA, Kew JNC, Wonnacott S (2008) Presynaptic α7- and β2-containing nicotinic acetylcholine receptors modulate excitatory amino acid release from rat prefrontal cortex nerve terminals via distinct cellular mechanisms. Mol Pharmacol 74:348–359. https://doi.org/10.1124/mol.108.046623
30. Zoli M, Pucci S, Vilella A, Gotti C (2018) Neuronal and extraneuronal nicotinic acetylcholine receptors. Curr Neuropharmacol 16:338–349. https://doi.org/10.2174/1570159x15666170912110450
31. Corradi J, Bouzat C (2016) Understanding the bases of function and modulation of α7 nicotinic receptors: implications for drug discovery. Mol Pharmacol 90:288–299
32. Buckingham SD, Jones AK, Brown LA, Sattelle DB (2009) Nicotinic acetylcholine receptor signalling: roles in alzheimer's disease and amyloid neuroprotection. Pharmacol Rev 61:39–61
33. Treinin M, Papke L, Nizri E et al (2017) Role of the α7 nicotinic acetylcholine receptor and RIC-3 in the cholinergic anti-inflammatory pathway. Cent Nerv Syst Agents Med Chem. https://doi.org/10.2174/1871524916666160829114533
34. Mizrachi T, Marsha O, Brusin K et al (2021) Suppression of neuroinflammation by an allosteric agonist and positive allosteric modulator of the α7 nicotinic acetylcholine receptor GAT107. J Neuroinflammation. https://doi.org/10.1186/S12974-021-02149-4
35. Pucci S, Fasoli F, Moretti M et al (2021) Choline and nicotine increase glioblastoma cell proliferation by binding and activating α7- and α9- containing nicotinic receptors. Pharmacol Res. https://doi.org/10.1016/J.PHRS.2020.105336
36. Hajiasgharzadeh K, Sadigh-Eteghad S, Mansoori B et al (2019) Alpha7 nicotinic acetylcholine receptors in lung inflammation and carcinogenesis: friends or foes? J Cell Physiol 234:14666–14679. https://doi.org/10.1002/JCP.28220
37. Bouzat C, Bartos M, Corradi J, Sine SM (2008) The interface between extracellular and transmembrane domains of homomeric Cys-loop receptors governs open-channel lifetime and rate of desensitization. J Neurosci 28:7808–7819. https://doi.org/10.1523/JNEUROSCI.0448-08.2008
38. Chrestia JF, Bruzzone A, del Esandi MC, Bouzat C (2021) Tyrosine phosphorylation differentially fine-tunes ionotropic and metabotropic responses of human α7 nicotinic acetylcholine receptor. Cell Mol Life Sci 78:5381–5395. https://doi.org/10.1007/S00018-021-03853-3
39. Young GT, Zwart R, Walker AS et al (2008) Potentiation of α7 nicotinic acetylcholine receptors via an allosteric transmembrane site. Proc Natl Acad Sci 105:14686–14691. https://doi.org/10.1073/pnas.0804372105
40. daCosta CJB, Free CR, Corradi J et al (2011) Single-channel and structural foundations of neuronal α7 acetylcholine receptor potentiation. J Neurosci 31:13870–13879. https://doi.org/10.1523/JNEUROSCI.2652-11.2011
41. Nielsen BE, Bermudez I, Bouzat C (2019) Flavonoids as positive allosteric modulators of α7 nicotinic receptors. Neuropharmacology. https://doi.org/10.1016/j.neuropharm.2019.107794
42. Lasala M, Fabiani C, Corradi J et al (2019) Molecular modulation of human α7 nicotinic receptor by amyloid-β peptides. Front Cell Neurosci. https://doi.org/10.3389/FNCEL.2019.00037
43. Andersen N, Corradi J, Sine SM, Bouzat C (2013) Stoichiometry for activation of neuronal α7 nicotinic receptors. Proc Natl Acad Sci USA 110:20819–20824. https://doi.org/10.1073/pnas.1315775110
44. Colquhoun D, Sigworth F (1995) Fitting and statistical analysis of single-channel records. In: Sakmann Bert, Neher Erwin (eds) Single-channel recording, 2 edn. pp 483–587, Boston, MA, US
45. Andersen ND, Nielsen BE, Corradi J et al (2016) Exploring the positive allosteric modulation of human α7 nicotinic receptors from a single-channel perspective. Neuropharmacology 107:189–200. https://doi.org/10.1016/j.neuropharm.2016.02.032
46. Ghovanloo MR, Ruben PC (2022) Cannabidiol and sodium channel pharmacology: general overview, mechanism, and clinical implications. Neuroscientist. https://doi.org/10.1177/10738584211017009
47. Nielsen BE, Minguez T, Bermudez I, Bouzat C (2018) Molecular function of the novel α7β2 nicotinic receptor. Cell Mol Life Sci 75:2457–2471. https://doi.org/10.1007/s00018-017-2741-4
48. Larsen HM, Hansen SK, Mikkelsen JD et al (2019) Alpha7 nicotinic acetylcholine receptors and neural network synaptic transmission in human induced pluripotent stem cell-derived neurons. Stem Cell Res. https://doi.org/10.1016/J.SCR.2019.101642
49. King JR, Ullah A, Bak E et al (2018) Ionotropic and metabotropic mechanisms of allosteric modulation of α 7 nicotinic receptor intracellular calcium. Mol Pharmacol 93:601–611. https://doi.org/10.1124/MOL.117.111401
50. Gilbert D, Lecchi M, Arnaudeau S et al (2009) Local and global calcium signals associated with the opening of neuronal alpha7 nicotinic acetylcholine receptors. Cell Calcium 45:198–207. https://doi.org/10.1016/J.CECA.2008.10.003
51. Zanetti SR, Ziblat A, Torres NI et al (2016) Expression and functional role of α7 nicotinic receptor in human cytokine-stimulated natural killer (NK) cells. J Biol Chem 291:16541–16552. https://doi.org/10.1074/jbc.M115.710574
52. Bouzat C, Sine SM (2018) Nicotinic acetylcholine receptors at the single-channel level. Br J Pharmacol 175:1789–1804
53. Neher E, Steinbach JH (1978) Local anaesthetics transiently block currents through single acetylcholine-receptor channels. J Physiol 277:153–176. https://doi.org/10.1113/JPHYSIOL.1978.SP012267
54. Yang KH, Galadari S, Isaev D et al (2010) The nonpsychoactive cannabinoid cannabidiol inhibits 5-hydroxytryptamine3A receptor-mediated currents in Xenopus laevis oocytes. J Pharmacol Exp Ther 333:547–554. https://doi.org/10.1124/JPET.109.162594
55. Hurst RS, Hajós M, Raggenbass M et al (2005) A novel positive allosteric modulator of the alpha7 neuronal nicotinic acetylcholine receptor: in vitro and in vivo characterization. J Neurosci 25:4396–4405. https://doi.org/10.1523/JNEUROSCI.5269-04.2005
56. Williams DK, Wang J, Papke RL (2011) Investigation of the molecular mechanism of the α7 nicotinic acetylcholine receptor positive allosteric modulator PNU-120596 provides evidence for two distinct desensitized states. Mol Pharmacol 80:1013–1032. https://doi.org/10.1124/MOL.111.074302
57. Ghovanloo MR, Choudhury K, Bandaru TS et al (2021) Cannabidiol inhibits the skeletal muscle Nav1.4 by blocking its pore and by altering membrane elasticity. J Gen Physiol. https://doi.org/10.1085/JGP.202012701
58. Ghovanloo MR, Shuart NG, Mezeyova J et al (2018) Inhibitory effects of cannabidiol on voltage-dependent sodium currents. J Biol Chem 293:16546–16558. https://doi.org/10.1074/JBC.RA118.004929
59. Fouda MA, Ruben PC (2021) Protein kinases mediate anti-inflammatory effects of cannabidiol and estradiol against high glucose in cardiac sodium channels. Front Pharmacol. https://doi.org/10.3389/FPHAR.2021.668657
60. Sreevalsan S, Joseph S, Jutooru I et al (2011) Induction of apoptosis by cannabinoids in prostate and colon cancer cells is phosphatase dependent. Anticancer Res 31:3799–3807
61. Komal P, Gudavicius G, Nelson CJ, Nashmi R (2014) T-cell receptor activation decreases excitability of cortical interneurons by inhibiting α7 nicotinic receptors. J Neurosci 34:22–35. https://doi.org/10.1523/JNEUROSCI.2093-13.2014

62. Sait LG, Sula A, Ghovanloo MR et al (2020) Cannabidiol interactions with voltage-gated sodium channels. Elife 9:1–17. https://doi.org/10.7554/ELIFE.58593
63. Lynagh T, Lynch JW (2012) Molecular mechanisms of Cys-loop ion channel receptor modulation by ivermectin. Front Mol Neurosci. https://doi.org/10.3389/FNMOL.2012.00060
64. Sauguet L, Howard RJ, Malherbe L et al (2013) Structural basis for potentiation by alcohols and anaesthetics in a ligand-gated ion channel. Nat Commun. https://doi.org/10.1038/NCOMMS2682
65. Zhao Y, Liu S, Zhou Y et al (2021) Structural basis of human α7 nicotinic acetylcholine receptor activation. Cell Res 31:713. https://doi.org/10.1038/S41422-021-00509-6
66. Dajas-Bailador FA, Mogg AJ, Wonnacott S (2002) Intracellular Ca2+ signals evoked by stimulation of nicotinic acetylcholine receptors in SH-SY5Y cells: contribution of voltage-operated Ca2+ channels and Ca2+ stores. J Neurochem 81:606–614
67. Guerra-Álvarez M, Moreno-Ortega AJ, Navarro E et al (2015) Positive allosteric modulation of alpha-7 nicotinic receptors promotes cell death by inducing Ca^{2+} release from the endoplasmic reticulum. J Neurochem 133:309–319. https://doi.org/10.1111/jnc.13049
68. Wu C-H, Lee C-H, Ho Y-S (2011) Nicotinic acetylcholine receptor-based blockade: applications of molecular targets for cancer therapy. Clin Cancer Res 17:3533–3541. https://doi.org/10.1158/1078-0432.CCR-10-2434
69. Pepper C, Tu H, Morrill P et al (2017) Tumor cell migration is inhibited by a novel therapeutic strategy antagonizing the alpha-7 receptor. Oncotarget 8:11414–11424. https://doi.org/10.18632/oncotarget.14545
70. Ahrens J, Demir R, Leuwer M et al (2009) The nonpsychotropic cannabinoid cannabidiol modulates and directly activates alpha-1 and alpha-1-Beta glycine receptor function. Pharmacology 83:217–222. https://doi.org/10.1159/000201556
71. Isaev D, Shabbir W, Dinc EY et al (2022) Cannabidiol inhibits multiple ion channels in rabbit ventricular cardiomyocytes. Front Pharmacol. https://doi.org/10.3389/FPHAR.2022.821758
72. Watkins AR (2019) Cannabinoid interactions with ion channels and receptors. Channels (Austin) 13:162–167. https://doi.org/10.1080/19336950.2019.1615824
73. Lodzki M, Godin B, Rakou L et al (2003) Cannabidiol-transdermal delivery and anti-inflammatory effect in a murine model. J Control Release 93:377–387. https://doi.org/10.1016/J.JCONREL.2003.09.001
74. Varvel SA, Wiley JL, Yang R et al (2006) Interactions between THC and cannabidiol in mouse models of cannabinoid activity. Psychopharmacology 186:226–234. https://doi.org/10.1007/S00213-006-0356-9